Exploiting the nonlinear impact dynamics of a single-electron shuttle for highly regular current transport

Michael J. Moeckel
Max-Planck-Institut für Quantenoptik, Hans-Kopfermann-Str. 1, 85748 Garching, Germany

Darren R. Southworth and Eva M. Weig
Center for NanoScience (CeNS) and Fakultät für Physik,
Ludwig-Maximilians-Universität, Geschwister-Scholl-Platz 1, München 80539, Germany

Florian Marquardt
Institute for Theoretical Physics, Universität Erlangen-Nürnberg, Staudtstr. 7, 91058 Erlangen, Germany

The nanomechanical single-electron shuttle is a resonant system in which a suspended metallic island oscillates between and impacts at two electrodes. This setup holds promise for one-by-one electron transport and the establishment of an absolute current standard. While the charge transported per oscillation by the nanoscale island will be quantized in the Coulomb blockade regime, the frequency of such a shuttle depends sensitively on many parameters, leading to drift and noise. Instead of considering the nonlinearities introduced by the impact events as a nuisance, here we propose to exploit the resulting nonlinear dynamics to realize a highly precise oscillation frequency via synchronization of the shuttle self-oscillations to an external signal.

Introduction. – Micro- and nanoscale resonators [1, 2] currently receive much attention both in applied and basic research. Their extreme sensitivity and design flexibility have enabled, for instance, mass sensing on the single ad-atom level [3–5], force sensitivity below the attonewton range [6, 7], and access to the ultimate quantum mechanical limits of motion [8–10]. Within this world of extremes, nanomechanical electron shuttles [11] have the potential to administer current with single-electron accuracy. This ultimate limit of current control would allow redefinition of the current standard [12–14], closing the metrological triangle by joining voltage and resistance as exact quantities defined in terms of fundamental constants.

A nanomechanical electron shuttle [15–22] consists of a nanomechanical resonator carrying a metallic island which oscillates between two metallic electrodes (Fig. 1). The island defines a quantum dot which, if operated in the Coulomb blockade regime [23, 24], can be consistently charged with a known number of charge carriers down to the single electron level. The advantage of nanomechanical shuttles over other single electron tunneling approaches is their inherent suppression of unwanted cotunneling due to tunnel contact with only one electrode at a time. Given sufficiently large DC voltage, the shuttle enters into Coulomb attraction-driven self-oscillation, where Coulombic forces suffice to drive the charged island to impact with and re-charge on subsequent electrodes [18, 19, 22], realizing a nanoscale version of Benjamin Franklin's "lightning bell" [25].

Going beyond the dynamical effects of the alternating recharging of the shuttle at the electrodes [26, 27], we model the highly non-linear (and less explored) motion in the impacting regime. We show that the impact dynamics can be exploited to provide a stable and reproducible frequency by synchronizing the self-oscillations to an external drive. In combination with charge quantization [20, 21], this will provide the desired reproducibility and precision of the shuttle current.

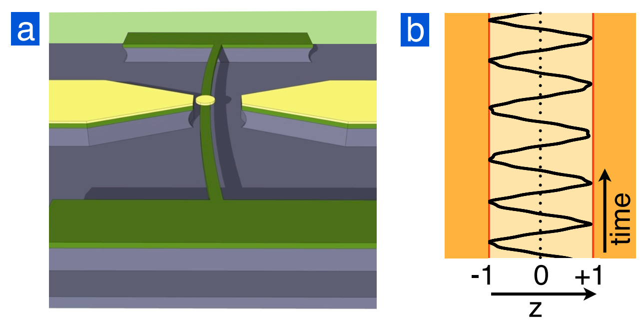

Figure 1: (a) A nanomechanical electron shuttle oscillating between two electrodes. (b) A typical trajectory of a shuttle driven by an oscillating force and impacting on the two electrodes.

Model. – The shuttle can be modeled as a nanomechanical harmonic oscillator with eigenfrequency ω_0, effective mass m, and quality factor $\mathcal{Q} = \omega_0/\Gamma$. We note that any extra intrinsic nonlinearities, while possibly present, do not alter the essential results below, since the main nonlinearity is provided by the impacts at the electrodes. The synchronization we analyze is a robust phenomenon, insensitive in its main aspects to many details of the model. The shuttle itself is centered halfway between two electrodes that are located at positions $\pm L$ and restrain its oscillatory motion. Thus, inelastic *impact events* occur at the electrodes, where the velocity reverses sign and is reduced by an impact damping parameter $\sqrt{\eta} \leq 1$. At the same time, the shuttle is charged to a value $q = \pm CV$

(depending on which electrode it contacts), and afterwards is accelerated towards the other electrode by a force $F = qV/2L \propto V^2$. A crucial component of our discussion is additional external driving, e.g. by a periodic force.

The motion between the electrodes is represented by the following equation of motion (written in dimensionless units):

$$\ddot{z}(\tau) + \mathcal{Q}^{-1}\dot{z}(\tau) + z(\tau) = \mathcal{F}\cos(\Omega\tau) \pm \mathcal{V}^2 \,. \qquad (1)$$

Position z and time τ are related to real physical units by $x = Lz$ and $\tau = \omega_0 t$. Impacts occur at $z = \pm 1$, where some kinetic energy will be lost, effectively re-scaling the velocity $v = \dot{z}$: $v' \equiv -\sqrt{\eta}v$. The force term $\mathcal{V}^2$ in Eq. (1) carries a sign that depends on which electrode has been contacted last ("+" for $z = -1$).

Our model is described by five dimensionless parameters: In Eq. (1), we introduce (i) the mechanical quality factor $\mathcal{Q}$, (ii) the dimensionless amplitude $\mathcal{F}$ of the external driving force, (iii) its external driving frequency Ω, written in units of the oscillator resonance frequency ω_0, (iv) the impact damping parameter η and (v) the dimensionless voltage $\mathcal{V} \equiv V/V_*$ with $CV_*^2/2 = m\omega_0^2 L^2$. The quantity $\mathcal{V}^2 = (V/V_*)^2$ is half the ratio between the charging energy and the oscillator's potential energy at the impact point. Note that in writing down Eq. (1) we assume the charge q to be linear in the voltage V. At low temperatures, in the Coulomb blockade regime, the charge shows discrete plateaus as a function of V. Then $\mathcal{V}^2$ in Eq. (1) and in all of the subsequent formulas and figures must simply be replaced by $QV/(2m\omega_0 L^2)$. Figure 1 displays a typical trajectory with impact at the electrodes, under simultaneous driving.

All the physical quantities of interest may be expressed by the dimensionless parameters and a few dimensional quantities. For example, the average shuttle current can be obtained from the transported charge CV and the frequency: $I = CV\omega_0\overline{\tau}^{-1}$. Here $\overline{\tau}^{-1}$ is defined as the averaged inverse (dimensionless) time for a one-way trip between the electrodes.

Self-oscillations without external driving. – When a sufficiently large dc voltage is applied to the electrodes, the shuttle can execute self-oscillations even in the absence of external resonant driving [11]. This happens when the acceleration by the electric field overcomes the frictional losses which are mostly due to the impact damping. While the existence of this regime is well-known, we will discuss it here, since its properties are crucial for our subsequent analysis. In this regime, the shuttle shows regular motion, where the velocity before impact is always the same. We first assume intrinsic oscillator losses to be absent (i.e. $\mathcal{Q} = \infty$, but $\eta \neq 0$). The energy lost upon impact is obtained via the relation $v' = \sqrt{\eta}v$ between the speeds before (v) and after (v') impact: $(v^2 - v'^2)/2 = v^2(1-\eta)/2$. This must equal the energy gained by acceleration in the electric field, $2\mathcal{V}^2$ in our units. Equating the two yields the velocity before impact:

$$v^2 = 4\mathcal{V}^2/(1-\eta) \,. \qquad (2)$$

Now we can obtain the one-way travel time τ_0. We assume the last impact was at $z(0) = -1$, with $\dot{z}(0^+) = v'$. Based on the solution $z(\tau) = \mathcal{V}^2 + v'\sin(\tau) - (1 + \mathcal{V}^2)\cos(\tau)$, we demand $z(\tau_0) = +1$. This yields τ_0 via $\sin\tau_0 = [-B + \sqrt{B^2 - 4AC}]/2A$, with $A = v'^2 + (1+\mathcal{V}^2)^2$, $B = 2v'(\mathcal{V}^2 - 1)$, and $C = -4\mathcal{V}^2$.

We note the following important physical features. Despite the impact damping, self-oscillations are possible down to the lowest voltages for $\mathcal{Q} = \infty$, because the grazing impact of the shuttle minimizes the loss: impact velocity $v \to 0$ for $\mathcal{V} \to 0$. In this limit, the one-way travel time is just half the intrinsic oscillator period ($\tau_0 = \pi$), i.e. the impact happens exactly at the turning point of the oscillatory motion, with the shuttle barely touching the electrode. Consequently, τ_0 then turns out to be independent of the impact damping parameter η. For *small voltages*, we obtain $\pi - \tau \approx 2\mathcal{V}(1+\sqrt{\eta})/\sqrt{1-\eta}$. This relation represents the decrease of the travel time from its zero-voltage value, to first order in $\mathcal{V}$, and it could serve to extract the impact damping η. At *high voltages* ($\mathcal{V} \gg 1$), one would observe $I \propto \mathcal{V}^2$, as higher accelerations lead to shorter travel times. However, current experimental parameters [22] indicate that typically $\mathcal{V}^2 \lesssim 10^{-2}$, which suggests that the high-voltage regime is not reached.

We now reconsider the intrinsic oscillator damping (thus $\mathcal{Q} < \infty$), where a minimum voltage has to be applied for self-oscillations [11, 24] in order to overcome the frictional losses. This voltage can be obtained by demanding the total loss (both by impact damping and mechanical friction) during one half-cycle to equal the energy gain by electrostatic acceleration. This then defines the threshold dc voltage for the shuttle's self-oscillations in the absence of driving:

$$\mathcal{V}_{\mathrm{thr}}^2 = \frac{\pi}{4}\mathcal{Q}^{-1} \,. \qquad (3)$$

Numerical calculations for the experimentally relevant parameters suggest that apart from the appearance of this threshold voltage there is no appreciable modification of the shuttle dynamics above threshold as long as $\mathcal{Q}$ is large [22].

General nonlinear map in the presence of driving. – Much more complex nonlinear behavior can be observed in the presence of an additional oscillatory drive, where several different attractors or even chaotic motion at higher drive strengths may arise.

Suppose an impact occurs at $z = -1$, with an initial velocity v_n. Once we also specify the phase $\varphi_n = \Omega\tau^{(n)}$ of the external oscillating force at the time $\tau^{(n)}$ of impact,

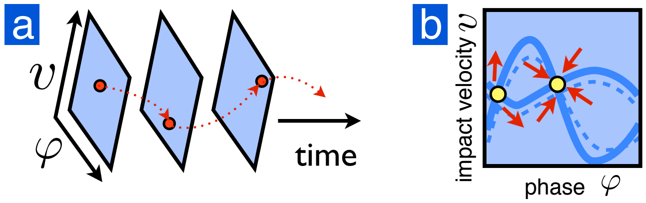

Figure 2: Nonlinear map for the impact dynamics of an electron shuttle. Phase φ of the external drive and impact velocity v are displayed at each impact event. (a) The evolution maps (φ_n, v_n) into (φ_{n+1}, v_{n+1}) upon the next impact at the same electrode. This map completely encodes the dynamics. (b) Fixed-points, both attractive and repulsive, arise in the (φ, v)-plane for suitable parameters. These are intersections of the curves where $v_{n+1} = v_n$ or $\varphi_{n+1} = \varphi_n$ (shown here). Small parameter changes usually do not change the number and type of fixed points, which makes synchronization robust.

these two values $(v_n,\ \varphi_n)$ completely determine the subsequent shuttle evolution. Evolving the shuttle towards the next impact at $z = -1$ (usually with an intermediate impact at $z = 1$), we find new values φ_{n+1} and v_{n+1}, which are determined by a unique mapping (cf. Fig. 2):

$$\varphi_{n+1} = \varphi'(\varphi_n, v_n) \tag{4}$$
$$v_{n+1} = v'(\varphi_n, v_n) \tag{5}$$

It is known that such two-dimensional nonlinear mappings can generate both complex attractors with a period larger than one cycle and chaotic dynamics. Below, we will be interested in synchronization, which (in the simplest case) is described by a period-one fixed point of the type $\tilde{\varphi} = \varphi'(\tilde{\varphi}, \tilde{v})$, $\tilde{v} = v'(\tilde{\varphi}, \tilde{v})$. Note that in the absence of an external drive, there would be only a one-dimensional relation $v_{n+1} = v'(v_n)$ which goes into a simple fixed-point. That is the regular shuttling already discussed above.

Synchronization to an external drive. – Although the map of Eqs. (4, 5) can generate a wealth of phenomena, our analysis below focuses on the case of greatest potential impact for applications. This is synchronization to an external drive (injection locking), which may be exploited to lock the shuttle dynamics to a very precise external frequency source even for a rather weak drive. In this way the nonlinear dynamics can be turned from a complication into a useful tool.

At small external driving strength, there is no simple fixed-point. This is because the phase just proceeds according to $\varphi_{n+1} \approx \varphi_n + 2\Omega\tau_0$, with τ_0 the one-way travel time in the absence of driving. Generally, $2\tau_0\Omega$ is not an integer multiple of 2π, and so there is no definite phase relation between the external driving and the shuttling. The combination of the shuttle's impact dynamics and the weak incommensurate driving makes the shuttle motion lose its exact periodicity. As a result, the shuttle's round-trip time $2\tau_0$ effectively changes slightly from step to step. Fig. 3a depicts the phase increment $\varphi_{n+1} - \varphi_n$ as a function of time and shows long-term beating patterns. However, when changing the shuttle's parameters (e.g. the voltage), the shuttle's intrinsic period shifts until it becomes almost commensurate with the external drive frequency. Then synchronization may set in (Fig. 3).

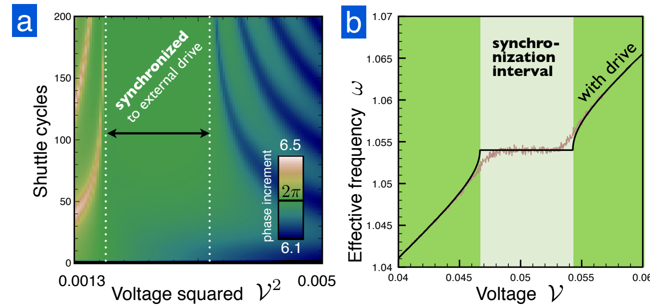

Figure 3: Synchronization of an impacting electron shuttle to an external drive. (a) The phase increment $\varphi_{n+1} - \varphi_n$ of the external drive between two impacting events is shown as a color-code. As time progresses (vertical axis, measured in shuttle cycles), the phase increment either displays a slow beating pattern, or it may lock to a value of 2π, signalling synchronization. This happens inside a certain interval, as the dc shuttle voltage (or any other parameter) is varied, shifting the shuttle's eigenfrequency. $[\eta = 0.2,\ \mathcal{Q} = 10^3,\ \mathcal{F} = 10^{-3},\ \Omega = 1.054\ ]$ (b) The effective, time-averaged shuttle frequency $\omega = \pi/\bar{\tau}$ is plotted vs. an external parameter (the voltage). Inside the synchronization interval, the shuttle becomes robust against noise (brown curve) – the curve shown here was obtained for fluctuations $\Delta\Omega = 0.02$ in the driving frequency (see main text) and is evaluated after 6000 impact events. The fluctuations decrease for longer averaging times.

Mathematically, this corresponds to the generation of a stable period-one fixed point. We now examine the appearance of this phenomenon both numerically and analytically. Numerical observations indicate that the system, once started anywhere in the (φ, v)-plane, quickly relaxes to a 1d manifold that can be described by the phase coordinate alone (Fig. 4a). Therefore, we focus on the phase map and expand it as

$$\varphi_{n+1} = \varphi_n + 2\Omega\tau_0 + K\sin(\varphi_n - \varphi_*) + \dots . \tag{6}$$

Here the values of K and φ_* depend on the detailed microscopic parameters, with the coupling K growing from zero upon increasing the drive, and the omitted terms are higher harmonics. Let us denote the deviation of the drive frequency from the undriven shuttling frequency as $\delta\Omega = \Omega - \pi/\tau_0$. If this is small enough, then we obtain a fixed point $(\varphi_{n+1} = \varphi_n = \tilde{\varphi})$, with some phase lag $\tilde{\varphi}$ between shuttling and drive, where $2\tau_0\delta\Omega = K\sin(\tilde{\varphi} - \varphi_*)$. This requires $|2\Omega\tau_0 - 2\pi| = |2\delta\Omega\tau_0| < K$, which defines the synchronization interval, i.e. the permissible deviation $\delta\Omega$. Outside that interval, the phase drifts across the full range $[0, 2\pi]$, with a varying velocity. Near synchronization, we can assume small phase increments, and

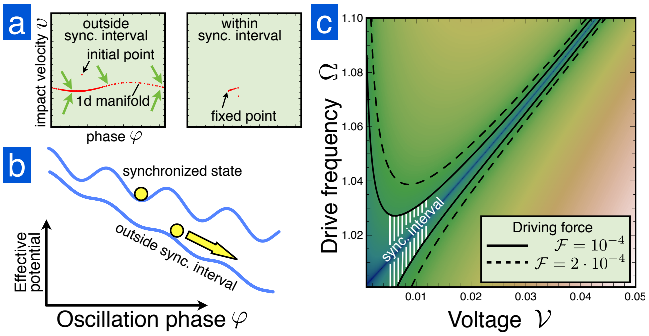

Figure 4: Phase dynamics in an impacting electron shuttle. (a) After only a few impact events, the system dynamics quickly settles onto a 1d manifold, permitting a theory for the phase dynamics alone. (b) The resulting Adler equation corresponds to a particle sliding in a washboard potential. (c) The predicted synchronization interval (bounded by the contour lines shown here, partially hatched) as a function of drive frequency, plotted using our approximate analytical prediction for the effective Adler coupling constant of a driven impact shuttle, Eq. (7). [$\eta = 0.7$]

the phase map of Eq. (6) can be written as a differential equation by replacing $\varphi_{n+1} - \varphi_n - 2\pi \approx 2\tau_0 d\varphi/d\tau$, introducing the time-dependent phase shift $\varphi(\tau)$. This yields a generic equation proposed by Adler to treat phase-locking phenomena [28, 29]. Integrating the Adler equation exactly one finds periodic dynamics for the phase increment in each cycle, with a period diverging as $|2\tau_0\delta\Omega - K|^{-1/2}$ near synchronization. All of this can be observed in the direct simulations (Fig. 3) of the nonlinear shuttle dynamics under drive and dc voltage. Outside the synchronization interval we see a periodic modulation with the period diverging near the onset of synchronization, as predicted.

While Adler-type equations appear generically in synchronization physics, they becomes predictive only when we are able to connect the coupling K to the microscopic parameters of the specific model. To this end we repeat the calculation of the one-way travel time for the driven oscillator, obtaining the correction $\delta\tau$ to the travel time τ_0 in the leading order of the driving $\mathcal{F}$. This also involves finding the change in the impact velocity by a new self-consistency equation, where we exploit the fact mentioned above that the velocity quickly relaxes to the limit cycle while the phase dynamics are much slower. We omit the rather lengthy calculation and just state that $\delta\tau$ becomes a harmonic function of φ. The corresponding correction to the phase increment is then $\delta\varphi = 2\Omega\delta\tau(\varphi)$. From this, we obtain the Adler coupling constant K:

$$K = \frac{\mathcal{F}}{2v}\left|e^{i\tau_0} - 1\right|\left|g\sqrt{\eta}\frac{MU - v_0\tilde{U}}{1-\sqrt{\eta}(\cos(\tau_0) - Mg)} - U\right| \quad (7)$$

Here $v = 2\mathcal{V}/\sqrt{1-\eta}$ is the impact velocity without drive (see above), and we abbreviated $U \equiv e^{i\tau_0}\tau_0 - \sin(\tau_0)$, $\tilde{U} \equiv 2e^{i\tau_0} - \cos(\tau_0)$, $g \equiv \sin(\tau_0)/v$, and $M \equiv -v'\sin(\tau_0) + (1+\mathcal{V}^2)\cos(\tau_0)$. Note that Eq. (7) is given under the simplifying but realistic assumptions of large $\mathcal{Q} \gg 1$ and near-resonant driving $\Omega \approx 1$. We find that Eq. (7) accurately matches the numerical results for sufficiently low drive $\mathcal{F}$.

The synchronization interval is given by $|\delta\Omega| < K/(2\tau_0)$, growing linearly with drive strength. As can be seen in Fig. 4c, the synchronization interval grows for lower voltages (while shifting towards lower frequencies). At very small voltages, modifications occur due to intrinsic damping (finite $\mathcal{Q}$), which destroys the self-oscillations.

Stability against noise. – The existence of an extended synchronization interval implies an increased robustness of the shuttling against noise. Within this interval, the Adler equation corresponds to a phase particle trapped in a local minimum of a washboard potential (Fig. 4b). There the effective shuttle frequency is completely insensitive to a slow drift of system parameters (voltage, effective capacitance, damping, etc.). In contrast, time-dependent noise may give rise to phase slips by lifting the particle over the barrier. However, this process is exponentially suppressed when moving towards the middle of the synchronization plateau [30]. We have confirmed this by direct simulation, for both (i) a noisy driving frequency Ω (reset at each impact to a new Gaussian random value) and (ii) a noisy impact parameter η. Our simulations do not show any noticeable effect of a noisy η on the synchronization range, even for $\Delta\eta/\langle\eta\rangle \sim \mathcal{O}(1)$. A leading-order perturbative calculation of the noise-induced correction to the one way travel time confirms the ineffectiveness of impact noise. For a noisy Ω we observe phase slips which drive the effective shuttle frequency ω away from $\langle\Omega\rangle$. They are numerous for voltages at the edges of the former synchronization interval. However, in the center of that interval (e.g. $\mathcal{V}$=0.053 in Fig. 3), for a noise value of $\Delta\Omega/\Omega = 0.02$, we observe no phase slips within 300,000 iterations, resulting in a frequency imprecision of at most 10^{-5} in this example. The remaining fluctuations of the effective time-averaged frequency ω decay with time as $1/\sqrt{\tau}$, as expected. Deviations of ω from the drive Ω are exponentially suppressed in the middle of the interval.

Realization. – Figure 1(a) depicts an experimental realization that strongly suppresses cotunneling events. Here, doubly-clamped, tensile-stressed silicon nitride string resonators with linear quality factors of several 100,000 [31, 32] can be be efficiently and controllably driven to sufficiently high (impacting) amplitudes of several 10nm using dielectric gradient field actuation [33] (acoustic [17] or capacitive drive [15, 16] can be used in similar contexts). Thus, during tunneling, the island is always tens of nanometers away from at least one electrode. The requirement that the charging energy dominates $k_B T$ can be satisfied with an island-electrode capacitance in the attofarad range, imposing experimentally accessible typical island cross sections of tens of nanometers. With these prerequisites within reach [17, 34], the ideas presented here would enable quantitatively reliable current measurements with a mechanical shuttle.

Conclusions. – In this Letter we have analyzed nanomechanical single electron shuttles in the impact regime. We predict that synchronization to an external driving frequency can occur and can be exploited to achieve a very precise shuttle current. This has immediate applications in the active experimental research on mechanical electron shuttles. In addition, the framework presented here can form the basis for discussing higher-order fixed-points and chaotic motion in shuttles and similar impacting systems.

Acknowledgments. - Financial support by the Deutsche Forschungsgemeinschaft via Projects No. Ko 416/18 (DS, EW), FOR 635 (MM), an Emmy-Noether grant, the German Excellence Initiative via the Nanosystems Initiative Munich (NIM) and LMUexcellent, as well as the European Commission under the FET-Open project QNEMS (233992) is gratefully acknowledged.

[1] A. N. Cleland, *Foundations of Nanomechanics* (Springer-Verlag Berlin Heidelberg New York, 2003).
[2] M. Poot and H. S. van der Zant, Physics Reports **511**, 273 (2012), ISSN 0370-1573.
[3] K. Jensen, K. Kim, and A. Zettl, Nature Nanotechnology **3**, 533 (2008).
[4] J. Chaste, A. Eichler, J. Moser, G. Ceballos, R. Rurali, and A. Bachtold, Nature Nanotechnology **7**, 301 (2012).
[5] M. S. Hanay, S. Kelber, A. K. Naik, D. Chi, S. Hentz, E. C. Bullard, E. Colinet, L. Duraffourg, and M. L. Roukes, Nature Nanotechnology **7**, 602 (2012).
[6] H. J. Mamin and D. Rugar, Applied Physics Letters **79**, 3358 (2001).
[7] D. Rugar, R. Budakian, H. J. Mamin, and B. W. Chui, Nature **430**, 329 (2004).
[8] A. D. O'Connell et al., Nature **464**, 697 (2010).
[9] J. D. Teufel et al., Nature **475**, 359 (2011).
[10] J. Chan et al., Nature **478**, 89 (2011).
[11] Gorelik, L. Y., Isacsson, A., Voinova, M. V., Kasemo, B., Shekhter, R. I., et al., Phys. Rev. Lett. **80**, 4526 (1998).
[12] M. W. Keller, J. M. Martinis, N. M. Zimmerman, and A. H. Steinbach, Applied Physics Letters **69**, 1804 (1996).
[13] J. P. Pekola, J. J. Vartiainen, M. Möttönen, O.-P. Saira, M. Meschke, and D. V. Averin, Nature Physics **4**, 120 (2008).
[14] B. Steck, A. Gonzalez-Cano, N. Feltin, L. Devoille, F. Piquemal, S. Lotkhov, and A. B. Zorin, Metrologia **45**, 482 (2008).
[15] Erbe, A., Weiss, C., Zwerger, W., Blick, and R. H., Phys. Rev. Lett. **87**, 096106 (2001).
[16] D. V. Scheible, C. Weiss, J. P. Kotthaus, and R. H. Blick, Physical Review Letters **93**, 186801 (2004).
[17] D. R. Koenig, E. M. Weig, and J. P. Kotthaus, Nature Nanotechnology **3**, 482 (2008).
[18] A. V. Moskalenko et al., Physical Review B **79**, 241403 (2009).
[19] H. S. Kim, H. Qin, and R. H. Blick, New Journal of Physics **12**, 033008 (2010).
[20] Y. Azuma, N. Kobayashi, S. Chorley, J. Prance, C. G. Smith, D. Tanaka, M. Kanehara, T. Teranishi, and Y. Majima, Journal of Applied Physics **109**, 024303 (2011).
[21] C. Kim, M. Prada, and R. H. Blick, ACS Nano **6**, 651 (2012).
[22] D. R. Koenig and E. M. Weig, Appl. Phys. Lett. **101**, 213111 (2012).
[23] H. Grabert and M. H. Devoret, *Single Charge Tunneling* (Plenum and New York, 1992).
[24] R. I. Shekhter, L. Y. Gorelik, M. Jonson, Y. M. Galperin, and V. M. Vinokur, Handbook of Theoretical and Computational Nanotechnology **5**, 1 (2006).
[25] B. Franklin, *The Papers of Benjamin Franklin and Vol. 5* (Yale University Press (New Haven) - 1962, 1753), chap. letter from Benjamin Franklin to Peter Collinson dated September 1753, p. 68.
[26] F. Pistolesi and R. Fazio, Phys. Rev. Lett. **94**, 036806 (2005).
[27] D. V. Scheible and R. H. Blick, New Journal of Physics **12**, 023019 (2010).
[28] R. Adler, Proceedings of the IRE **34**, 351 (1946).
[29] B. Razavi, IEEE Journal of Solid-State Circuits **39**, 1415 (2004).
[30] A. Pikovsky, M. Rosenblum, and J. Kurths, *Synchronization: A Universal Concept in Nonlinear Sciences*, Cambridge Nonlinear Science Series (Cambridge University Press, 2003), ISBN 9780521533522.
[31] S. S. Verbridge, J. M. Parpia, R. B. Reichenbach, L. M. Bellan, and H. G. Craighead, Journal of Applied Physics **99**, 124304 (2006).
[32] Unterreithmeier, Q. P., Faust, Thomas, Kotthaus, and J. P., Phys. Rev. Lett. **105**, 027205 (2010).
[33] Q. P. Unterreithmeier, E. M. Weig, and J. P. Kotthaus, Nature **458**, 1001 (2009).
[34] C. Weiss and W. Zwerger, Europhysics Letters (EPL) **47**, 97 (1999).